Hydrology and
Earth System
Sciences

Assessing the quality of digital elevation models obtained from mini unmanned aerial vehicles for overland flow modelling in urban areas

João P. Leitão, Matthew Moy de Vitry, Andreas Scheidegger, and Jörg Rieckermann

Eawag: Swiss Federal Institute of Aquatic Science and Technology, Überlandstrasse 133, 8600 Dübendorf, Switzerland

Correspondence to: João P. Leitão (joaopaulo.leitao@eawag.ch)

Abstract. Precise and detailed digital elevation models (DEMs) are essential to accurately predict overland flow in urban areas. Unfortunately, traditional sources of DEM, such as airplane light detection and ranging (lidar) DEMs and point and contour maps, remain a bottleneck for detailed and reliable overland flow models, because the resulting DEMs are too coarse to provide DEMs of sufficient detail to inform urban overland flows. Interestingly, technological developments of unmanned aerial vehicles (UAVs) suggest that they have matured enough to be a competitive alternative to satellites or airplanes. However, this has not been tested so far. In this study we therefore evaluated whether DEMs generated from UAV imagery are suitable for urban drainage overland flow modelling. Specifically, 14 UAV flights were conducted to assess the influence of four different flight parameters on the quality of generated DEMs: (i) flight altitude, (ii) image overlapping, (iii) camera pitch, and (iv) weather conditions. In addition, we compared the best-quality UAV DEM to a conventional lidar-based DEM. To evaluate both the quality of the UAV DEMs and the comparison to lidar-based DEMs, we performed regression analysis on several qualitative and quantitative metrics, such as elevation accuracy, quality of object representation (e.g. buildings, walls and trees) in the DEM, which were specifically tailored to assess overland flow modelling performance, using the flight parameters as explanatory variables. Our results suggested that, first, as expected, flight altitude influenced the DEM quality most, where *lower flights* produce better DEMs; in a similar fashion, *overcast* weather conditions are preferable, but weather conditions and other factors influence DEM quality much less. Second, we found that for urban overland flow modelling, the UAV DEMs performed competitively in comparison to a traditional lidar-based DEM. An important advantage of using UAVs to generate DEMs in urban areas is their flexibility that enables more frequent, local, and affordable elevation data updates, allowing, for example, to capture different tree foliage conditions.

1 Introduction

1.1 Urban drainage modelling

Densely urbanised areas, where most economic activities take place, face higher probability of flood occurrence due to (i) the large percentage of impervious areas, which consequently increase the runoff volume; and (ii) alterations of natural water streams and existence of sewer systems, which increase flow velocities, thus reducing catchments' time of concentration and duration of the critical rainfall events. In addition, climate change may increase rainfall intensity and frequency in some regions of the globe, which will affect ecosystems and human life. These more frequent extreme conditions can ultimately increase the probability that urban drainage system capacity is exceeded, which may lead to higher urban flood risks (when flood consequences are maintained).

Hydrological and hydraulic models are important tools to estimate urban flood risk and help engineers and decision makers designing urban drainage systems that inherently reduce these risks. Urban drainage models should be represented by coupling the sewer system (one-dimensional model, 1-D) with the overland flow system (1-D or 2-D).

Several studies have tested and compared different urban drainage modelling approaches (e.g. Apel et al., 2009; Villanueva et al., 2008; Allitt et al., 2009), such as 1-D sewer system (e.g. Vojinović and Tutulić, 2009), coupled 1-D sewer system with 1-D overland flow system (1-D–1-D) (e.g. Maksimović et al., 2009; Leandro et al., 2009), and coupled 1-D sewer system with 2-D overland flow system (1-D–2-D) (e.g. Chen et al., 2007). The different coupled modelling approaches rely on the quality of the digital elevation model (DEM) to represent the terrain and then locate flood-prone areas – this is especially important for local (and more frequent) floods when compared to large floods (e.g. fluvial, coastal flooding, or a combination of these two types).

1.2 UAV applications and operational challenges

Unmanned aerial vehicles (UAVs) are reusable vehicles that fly without a pilot on board; therefore, their operation can be either autonomous, remote controlled, or a combination of the two. The range of applications of UAVs in the civil context is already vast, e.g. archaeology (Sauerbier and Eisenbeiss, 2010), precision agriculture (Zhang and Kovacs, 2012), and crowd monitoring (Duives et al., 2014). UAVs have, however, a strong negative connotation, which has motivated both civilian and military sectors to propose alternative names, such as remotely piloted aircraft (RPA) or unmanned vehicle system (UVS) (Bennett-Jones, 2014; Eisenbeiss, 2009). While their application in military operations was perhaps their first use, the industry of civil UAVs has been increasing steadily, as illustrated by the number of civil UAVs that has more than doubled since 2008 (Colomina and Molina, 2014). Applications of UAVs are also getting significant visibility in the media, mostly due to privacy (Vilmer, 2015; Wildi, 2015) and safety issues.

UAVs can take the form of single- or multiple-blade helicopters and fixed-wing aircraft, though other possibilities exist. Eisenbeiss (2009) gave an extensive historical background of the various UAV types. These different UAV forms incorporate different safety features in order to prevent injuries and damages in the event of a flight failure; these are for example, the incorporation of a parachute. In the case of the eBee UAV, used in this study, its extremely light frame and its gliding capability make it safe in the case of flight failure and hence safe to fly in urban areas. This safety issue is of course a serious concern of the public and of the managers of public space. To respond to this concern, different countries have legislation already in place or being prepared to regulate the public use of UAVs in urban areas and mass gathering events. Nevertheless, we consider that the use of UAVs for civil applications will continue to increase, thanks to the development and improvement of the unmanned aerial systems technology such as UAV, UAV control and navigation software, and sensor technology.

1.3 Urban drainage models' input elevation data and UAVs

From the literature, it is clear that a great effort has been made to develop new and improve existing numerical methods for hydraulic models. However, DEMs, as all input data, can also have a significant impact on overland flow modelling results (Fewtrell et al., 2011; Leitão et al., 2009). Leitão et al. (2009) showed the effect that DEM sources, resolution and accuracy have on the delineation of overland flow paths in urban catchments; fine-resolution DEMs are required to obtain accurate 1-D overland flow networks in urban areas. Fewtrell et al. (2011), who evaluated two different hydraulic models on a DEM of resolution varying from 0.5 to 5 m, also concluded that the data resolution has a greater effect on results than the model used, especially if not calibrated. While it is evident that the representation of roads is critical, requiring a minimum resolution of 2 to 3 m, walls and street curbs are also elements that influence the propagation of a flood wave (Sampson et al., 2012), but to represent these elements in the DEM, a finer resolution (< 1 m) is required. Realistic and detailed representation of terrain thus plays a fundamental role in overland flow modelling.

The recent developments of UAVs and their increasing availability make them a new potential source of terrain elevation data. The fine spatial resolution that can be obtained (e.g. 0.05 m) is well-suited to conduct detailed urban overland flow studies. Furthermore, thanks to the low cost of operation, UAVs make multiple flights feasible, thereby enabling the analysis of how different conditions, such as tree-leaves-off or tree-leaves-on conditions, affect the characterisation of impervious areas, which is important for urban flood modelling. The handling of UAVs is simplified to a degree that can be managed by non-expert professionals, such as civil engineers and engineering consultants. To our knowledge, this study is the first time DEMs produced with photogrammetry utilising UAV imagery (commonly called UAV photogrammetry) are used in the context of urban drainage, more specifically on overland flow modelling. Although experiments have been carried out using light detection and ranging (lidar) mounted on quadcopter type of UAVs, this is still not possible with the eBee UAV used in this study. Besides the issue of proprietary firmware, lidar equipment is heavier and consumes much more power than a camera needed to achieve similar resolution with photogrammetry. This makes it impractical when surveying significant areas of land (i.e. up to a few square kilometres for suburban catchments in Switzerland), further increasing the safety hazard in case of a crash.

1.4 Generation of very fine-resolution digital elevation models using UAV imagery

1.4.1 Photogrammetric process

Photogrammetry is often the preferred methodology when collecting 3-D data using UAVs. Photogrammetry produces 3-D point clouds based on overlapping images. Other useful by-products can be derived, such as urban façade textures (Leberl et al., 2010). For UAVs, photogrammetry is an interesting alternative to the predominant lidar method. lidar techniques are precise and allow for multi-returns – e.g. in areas with trees the ground elevation can be automatically measured. However, due to the weight and high-energy demand of lidar devices, they are not adequate for UAVs and impossible to use with mini UAVs. On the other hand, the images can be taken with light equipment (e.g. consumer cameras) that does not require high energy. The question of photogrammetry versus lidar has been raised and discussed in a few past publications (Baltsavias, 1999; Leberl et al., 2010; Strecha et al., 2011). Specific applications of UAV photogrammetry are presented in Remondino et al. (2011).

The main photogrammetry steps to generate 3-D elevation models from overlapping images are presented in Strecha et al. (2011):

1. Images are scanned for characteristic points, such as, for example, marks created in the ground specifically to support the survey or manholes. If ground control points (GCPs) are used to geo-reference the model, they are usually labelled in the images before this step.

2. Based on the characteristic points, image geo-information and the known camera parameters, a sparse point cloud model is derived with a so-called bundle block adjustment algorithm (Triggs et al., 2000). It is sparse since formed only of the characteristic points from step 1.

3. Based on the sparse point cloud, dense image matching is performed to increase the spatial resolution of the point cloud model and the 3-D elevation model generated.

1.4.2 Digital elevation model generation process

The resulting point cloud may contain errors, such as image shadows, mismatches, and lens distortion. Therefore, algorithms for outlier removal and smoothing can be applied. If a digital surface model (DSM) is required, vegetation, buildings, and other objects need to be filtered out. Finally, the resulting point cloud is triangulated to a triangulated irregular network (TIN), which may then be rasterised and used, for example, in hydraulic modelling software.

1.5 Study objectives

In this paper we aim at demonstrating the benefit of using high-resolution DEMs produced from mini UAV acquired data on urban drainage modelling, as opposed to DEMs based on standard aerial lidar elevation data. Specifically, our study presents three distinct novelties.

- First, to the best of our knowledge, it uses for the first time DEMs produced from UAV photogrammetry in the context of urban drainage – more specifically on overland flow modelling.

- Second, it presents dedicated field experiments specifically tailored to understand how UAV flight parameters affect DEM quality and, eventually, overland flow representation.

- Third, it compares the quality of the UAV obtained DEM with a DEM used by Swiss engineers (lidar-based DEM) and discusses advantages and disadvantages for urban drainage and flood modelling.

Our results suggested that UAVs are a very promising technology for our purpose and that results are relatively robust to not optimal flight parameters. Given the current developments, we expect that the quality of the products generated using these systems will quickly improve in the near future due to better software that manufacturers provide together with the UAV platforms. However, important limitations might arise from regulatory affairs. This will also be discussed below.

This paper is organised as follows: Sect. 2 describes the methods proposed in this study to evaluate the UAV DEM and assess the impact of flight parameters on DEM quality. In Sect. 3 the case study location and the flight parameters are presented; UAV and camera used are also described in this section. Analysis of findings are presented and discussed in Sect. 4. Finally, Sect. 5 summarises the major findings of the study, identifying also potential further research.

2 Methods

2.1 Impact of UAV flight parameters on DEM generation for overland flow modelling

The adequacy of a DEM for urban flood assessment cannot be defined objectively as the existing criteria (e.g. elevation, slope, or aspect differences to a benchmark DEM) are not specific to each of the possible DEM applications. As a pragmatic solution, we propose a set of four qualitative and four quantitative evaluation metrics to evaluate the DEM quality. First, DEM values were compared with field measurements using, for example mean absolute errors and visual classification. Second, two statistical models were developed to explore the relations between the flight parameters and the

Table 1. Qualitative metric classes.

Class	Representation of voids	Representation of buildings edges	Representation of walls	Presence of trees
3	100 % open	Sharp edges	Perfectly represented wall	Not visible
2	50 % open	Little noisy	A straight object	Freckles
1	25 % open	Very noisy	Unclear	Almost complete
0	0 % open	Chaotic	Nothing	Complete

DEM quality through the evaluation metrics: (i) an odds logistic regression model was applied for the qualitative metrics and (ii) a linear regression model was used to evaluate the quantitative metrics.

2.1.1 Qualitative metrics to assess DEM for overland flow modelling

Representation of voids between two closely located objects

This metric describes the space between two closely placed objects, such as buildings. This is an essential feature of a good-quality DEM for overland flow modelling, as in many flood events water flows through such small openings, which, consequently, can have a significant impact on the modelling results.

Quality of building edges representation

Building edges can be subject to distortions and to a "salt and pepper" effect caused by multiple 3-D points being identified one over the other; this is commonly associated with pixel-based classifications (De Jong et al., 2001). This metric describes the severity of building wall distortion and is important to assess the quality of the representation of linear features in the DEM, which can divert overland flow.

Representation of walls

Walls are very relevant for overland flow modelling because they can obstruct and redirect water movement. This metric describes to what extent these elements are represented in the DEM.

Presence of trees

This metric describes whether trees are represented in the DEM, or not. It is desirable not to have trees represented because tree canopies, which are what is represented in the DEMs, do not influence overland flow.

The qualitative metrics were calculated based on a visual analysis of the DEM; a class was assigned to each analysis location. The classes are on an ordinal scale, where class 0 is the least favourable and class 3 the best class (Table 1).

2.1.2 Quantitative metrics to assess DEM for overland flow modelling

The following quantitative metrics may be considered a first attempt to define objective evaluation criteria to assess DEM quality for overland flow modelling. The metrics aim to describe the deviations from the reality of the representation of terrain features that may influence overland flow.

Absolute elevation differences

The vertical correctness of the DEM is relevant for urban drainage modelling. Suitable reference elevation data can be surveying points and a sewer manhole cadastre. In our case study, the vertical precision of the surveying points was given for each point and varied between 0.5 and 3 cm (1σ). The vertical accuracy of the manholes is not known; however, it is assumed to have a standard deviation of 7.5 cm (VBS, 2008).

Curb height differences

The height difference between road and sidewalk is relevant for relatively low overland flow. Although runoff occurs all over the catchment area, overland flow tends to concentrate in roads in urban areas; for large runoff events (e.g. flooding events) the overland flow will flow over sidewalks. Curb heights can be measured repeatedly at various locations in the area of study. To assess the curb height from the different DEMs representing different flight parameters, the average elevation difference between $1\,m^2$ areas on the road and on the sidewalk close to the curb height measurement location was calculated.

Flow direction (i.e. terrain aspect)

Flow direction was measured on the field by pouring water and measuring orientation of flow direction with a compass (see Fig. 1a). In the DEM, the aspect was calculated, based on a 3×3 cell moving window (Burrough and McDonnell, 1998).

Flow path delineation

It is important that delineated flow paths are properly represented (mainly along the side of the roads), so that modelled overland flow runs into (or pass by in the vicinity of)

(a) Terrain aspect and flow path field experiment preparation

(b) Aerial photo of field experiment location

Figure 1. Example of the field experiments conducted to calculate the terrain flow direction and flow path delineation metrics.

sewer inlets. To assess the representativeness of the DEM-based delineated flow paths, real flow paths were observed by pouring water onto the road (Fig. 1a) and measuring the distance between the stabilised flow and the road curb (j in Fig. 1b). Often, the water flowed exactly on the side of the road. In the DEM, water flow paths were estimated using the flow accumulation method (Jenson and Domingue, 1988).

2.1.3 Statistical models

To identify the important flight parameters that determine DEM quality, two simple statistical models were used; one for the qualitative and a different one for the quantitative assessments.

Because the qualitative metrics are measured on an ordinal scale, the influence of the flight parameters was investigated with a proportional odds logistic regression model (see, e.g., Venables and Ripley, 2002). This model considers the natural order of the metrics, e.g. that class 3 is better than class 2. The probability that the jth observation of metric Y is at least as good as class k is modelled as

$$P\left(Y_j \leq k\right) = \frac{1}{1 + \exp\left(\varsigma_k - \eta_j\right)}, \tag{1}$$

where the thresholds $\varsigma_0 = -\infty < \varsigma_1 < \cdots < \varsigma_4 = \infty$ are coefficients that are estimated additionally to the *coefficients* of the linear predictor η_j, which is defined in Eq. (2).

For every quantitative metric, a linear regression model was set up to model the absolute differences between the values obtained from the DEM and the corresponding ones measured in the field

$$\eta_j = \beta_0 + \beta_1 z_{j1} + \beta_2 z_{j2} + \cdots + \beta_r z_{jr}, \tag{2}$$

$$Y_j = \eta_j + \epsilon_j, \tag{3}$$

where z_{jr} are the corresponding explanatory variables for the jth observation, ε is a Gaussian random error term and the $\beta_r, r = 0, 1, \ldots, r$ regression coefficients to be estimated. As explanatory variables all five flight parameters (i) flight altitude, (ii) camera pitch, (iii) frontal and (iv) lateral overlap, and (v) weather conditions (see Sect. 3.3) were used. As the *weather condition* provides qualitative information, it was included using dummy variables (see, e.g., Montgomery et al., 2012).

2.2 Comparison between a UAV DEM and a conventional lidar-based DEM

UAV systems are being used for relatively localised surveys, and these surveys are usually targeted to a specific application. The resolution of the imagery produced using UAVs is, in general, of very high resolution as the flying altitude is low. In the specific case of this study, the UAV DEM was generated based on photogrammetry. The lidar-based DEM used in this study covers the whole Switzerland and was obtained to be applied in multiple purposes. By definition, the flight altitude is much higher than that of the UAV, allowing one to cover larger areas in a reasonable amount of time. The lidar-based DEM was generated based on lidar technology, which is completely different from photogrammetry technique used to generate the UAV DEM.

From the general description above, one can say that the DEMs used for the comparison have distinct characteristics. However, the DEM comparison performed in this study is still valid as the analysis conducted in the study aims at comparing the two by practical use in engineering projects and not by technological standards or DEM generation methodologies.

Table 2. Characteristics of the 16 flights.

Flights	Flight altitude (m)	GSD (cm)	Camera pitch (°)	Frontal overlap (%)	Lateral overlap (%)	Weather conditions[b]
1	145	4.5	0	80	70	Clear
2	145	4.5	0	70	80	Clear
3	145	4.5	7	70	80	Clear
4[a]	145	4.5	15	70	80	Clear
5	205	6.5	0	70	80	Clear
6	205	6.5	7	70	80	Clear
7	205	6.5	15	70	80	Clear
8	85	2.5	0	70	80	Overcast
9	310	10	0	70	80	Partly cloudy
10	220	7	5	70	80	Clear
11	220	7	5	85	80	Partly cloudy
12	220	7	5	55	80	Clear
13	220	7	5	70	65	Clear
14	220	7	5	70	90	Clear
15	220	7	5	70	70	Clear
16	220	7	5	60	80	Partly cloudy

[a] DEM generated from flight 4 was used for the comparison with the lidar DEM;
[b] http://www.erh.noaa.gov/er/box/glossary.htm.

The UAV DEM was generated based on flight 4 data (see Table 2), after a thorough comparison of the different flights (Moy de Vitry, 2014), which showed the good quality of the DEM produced from this flight. The lidar DEM is a 3-D height model that covers the whole of Switzerland at a resolution of one data point per $2\,m^2$ and was then interpolated from the raw model to generate a 2 m raster grid. It is provided by Swisstopo[1] and represents all stable and visible landscape elements such as soil, natural cover, woods and all sorts of built infrastructure, such as buildings. The data acquisition method used is aerial lidar with a vertical accuracy of $\pm 0.5\,m$ (1σ) in open terrain, and in terrain with vegetation the vertical accuracy is $\pm 1.5\,m$ (1σ). The smallest UAV DEM pixel size was 5 cm, whereas the lidar DEM[2] had a pixel size of 2 m. Swisstopo lidar data are acquired in midsummer, but the detailed processing method of the data for creating the lidar DEM is not published.

To compare the two DEMs, we built on the work of Podobnikar (2009), who discussed various visual assessment methods for identifying problems in DEMs that are otherwise not measured, like discontinuities. We also used suggestions by Reinartz et al. (2010), who used elevation differences and several terrain properties, such as slope and land cover, to compare two DEMs. Specifically, we used the following metrics for this specific purpose:

a. visual DEMs comparison with hillshade[3];

b. elevation differences between the two DEMs for diverse land uses (absolute differences and mean absolute differences);

c. slope and aspect differences between the two DEMs. These two terrain surface characteristics are essential when considering overland flow modelling as they are associated with flow speed and direction;

d. delineation of flow paths: the flow paths were delineated using the D8 flow direction algorithm (Jenson and Domingue, 1988). This metric is meant to help understanding the correctness of overland flow representation.

To compute the values for metrics (b) and (c), the 2 m downsampled UAV DEM was used to match the resolution of the lidar DEM used in the comparison.

3 Material: UAV and case study

3.1 Unmanned aerial system

3.1.1 General

The mini UAV platform, called "eBee" (from year 2013) developed by senseFly, was used in this study. The eBee UAV

---

[1] http://www.swisstopo.admin.ch/internet/swisstopo/en/home/products/height/dom_dtm-av.html

[2] Swiss Federal Office of Topography (Article 30, Geoinformation Ordinance).

[3] A hillshade is a greyscale visualization of the 3-D surface, with a lateral light source.

(a) Adliswil (Zurich Canton, Switzerland)

(b) Case study areal aerial photo (130x300 m)

Figure 2. Case study location and area aerial photo.

is a fully autonomous fixed-wing electric-powered aircraft, with a wingspan of 0.96 m and weighs approximately 0.7 kg including a payload of 0.15 kg. The UAV can cover relatively large areas in a reasonable amount of time (maximum of $12 \, \text{km}^2$ per 50 min flight – this value is strongly related to flight altitude and, consequently, to maximum image resolution), which is important for the economic viability of UAV remote sensing. Detailed information about the UAV used in this study is presented in Appendix A.

We selected this specific unmanned aerial system over other platforms for two main reasons. First, it is delivered as a complete system with flight planning and photogrammetry software, designed to work seamlessly with one another in a straightforward and intuitive way and does not requiring flying expertise. Second, the construction of the UAV itself provides passive safety, because it is lightweight and electric powered, has a foam body and, most important, glides if out of power. In addition, the autopilot has built-in safety procedures, which is crucial for flights over urban areas.

3.1.2 Camera

The UAV was equipped with a customised Canon IXUS 127 HS that is triggered by the UAV autopilot. The camera has 16.1 Million Pixels with RGB bands and operates in auto mode, meaning that the photo exposure (e.g. speed and aperture) is automatically adjusted for each photo. Thus, it is not possible to configure the settings globally for a given flight; for that, a different camera would be required. Detailed characteristics of the camera are presented in Appendix A. With the eBee system, flight altitude is the main modulator for the ground sampling distance of images acquired. In Table 2, the reader can appreciate how flight altitude and GSD are related.

3.1.3 Photogrammetry software

The photogrammetry tasks, such as bundle block adjustment, point cloud generation and filtering were performed using the *Pix4D*[4] *software* (Strecha et al., 2011). This is one of the leading software for UAV photogrammetry (Sona et al., 2014); its main strength is a good handling of rather imprecisely referenced images like those acquired from lightweight UAVs.

3.2 The case study area

Adliswil is a city near Zurich (Switzerland) and was chosen to be the case study area mainly because (i) it is a typical, rapid growing Swiss city (approx. 20 000 inhabitants) that (ii) needed up-to-date elevation data to be used in other urban drainage studies. Six areas in Adliswil were initially considered and evaluated to conduct the UAV flights. The experimental area was selected based on several criteria related to overland flow, such as including different road types and sidewalks, different terrain types, significant terrain elevation difference, high road density and roads that are relatively free of cars. In addition, practical criteria, such space for UAV taking-off and landing, visibility of UAV during flight from the take-off point had to be considered. The chosen location has an area $0.04 \, \text{km}^2$ (approx. $130 \, \text{m} \times 300 \, \text{m}$) and is illustrated in Fig. 2. The case study location is outside the Swiss Air controlled zone[5]; hence, no permission was required to fly the UAV, as long as it always remained in line of sight.

---

[4]http://pix4d.com/
[5]http://www.skyguide.ch

3.3 Experimental field work: flights with different parameters

In total, 14 flights were conducted (flights 1 to 14) on the case study area to test the influence of flight parameters on the adequacy of DEMs for overland flow modelling. The flight parameters considered in this study are presented as follows.

Flight altitude

The flight altitude is one of the main factors that determines the scale and accuracy of the point cloud (Kraus, 2012); it is directly related to the ground sampling distance (GSD). Therefore it is expected that a low flight altitude will have a positive influence on the representation of the terrain details on DEMs. In theory, flight heights of up to 1000 m are possible with the eBee. There is no lower limit, although safety and image overlap (the camera frequency is limited) become issues below 70 m above ground. In Switzerland, line-of-sight flight is required by the legislation, which limits the maximum altitude that is typically reached in flight.

Camera pitch

Camera pitch can be assumed to have influence on the representation of steep surfaces; high values of camera pitch are assumed to generate better representations of steep surfaces, such as façades. While façades are of limited interest in urban drainage modelling, it is of interest to see whether camera pitch variation affects the representation of objects, such as cars or walls, which influence overland flow. With the eBee, the camera pitch can be defined between 0 and 15°.

Image overlap

Image overlap is expressed in percent for both frontal and lateral directions, and is an important parameter in the photogrammetric process. First, a high overlap increases redundancy of point identification, which improves the 3-D precision of the point cloud. Second, it reduces distortions in the orthophoto. In order to achieve acceptable matching between images, it is recommended to have a frontal overlap of 60 % or more. This lower limit should be increased in the case of complex terrain (for example forest), or in the case of unstable platforms (for example UAVs).

Weather conditions

Lighting and the presence of shadows may have a strong effect on photogrammetry results. We deliberately did not adjust the flight plans to weather conditions. All the flights took place within a 2-day time interval; some of the flights were performed under cloudy conditions whereas others were performed with direct sunlight.

The flights were conducted on 29 and 30 January 2014 between 11:30 and 13:30 LT (local time) (solar noon on those days was around 12:40 LT). In addition to the 14 flights, 2 virtual flights (flight 15 and flight 16) were generated from 2 of the 14 flights to simulate the effect of image overlapping. Flight 15 was generated from every third flight line of flight 14. Similarly, flight 16 was generated from every third image from flight 11. These two additional virtual flights were created to (i) increase the number of "flights" used in the statistical analysis with different parameters and (ii), specifically, to investigate the effect of image overlapping on the quality of UAV imagery DEMs. This contributed to a more robust statistical analysis of the impact of UAV flight parameters on DEM quality (based on the selected DEM evaluation metrics). The parameters of all 16 flights are presented in Table 2.

3.4 Surveying points

3.4.1 Georeferencing points

Five ground control points were used to geo-reference the digital elevation models (see Fig. 3). The control points used were official survey points (LFP3) with a vertical accuracy of 3.7 cm and a horizontal accuracy of 3 cm. Since the points are protected with access covers, it was the access covers that were used for georeferencing the images. It was assumed that the cadastral points were directly underneath the centre of their cover. For this reason, the elevation difference between the points and their covers was measured and compensated for (Fig. 3), but any horizontal discrepancies were neglected.

3.4.2 Data preparation

The settings that were used to generate the UAV DEMs with the Pix4D software for the steps of feature extraction, point cloud generation, and point cloud filtering are shown in Table 3. The reader can refer to the Pix4D user manual (Pix4D Support Team, 2014) for detailed information. For the assessment of the influence of UAV flight parameters on DEM quality, default settings were used. For the DEM comparison, settings were chosen through trial and error.

Co-registration of the UAV DEM with the lidar DEM is done implicitly by georeferencing the point clouds with the official survey points. By doing so, the generated UAV DEM is also georeferenced and can be directly overlaid with the lidar DEM, which is provided in the same coordinate reference system.

3.4.3 DEM quality assessment locations

Figure 4 presents the locations surveyed to then allow for calculating the (a) qualitative and (b) quantitative metrics.

Figure 3. Left: locations of the georeferencing points used in the study (red crosses). While the left-most points are outside of the area of study, they were covered by UAV images. Right: measurement of vertical distance between GCP access cover and actual GCP point.

(a) Qualitative assessment

(b) Quantitative assessment

Figure 4. Location used to calculate the metric values.

4 Results and discussion

In this section we first present the results of the influence of parameters on DEM quality, and second the results from the comparison of the UAV DEM to the lidar DEM.

4.1 Impact of UAV flight parameters on DEM generation for overland flow modelling

The statistical models set-up for the qualitative metrics showed that, as expected, lower flight altitude produces better DEMs for overland flow modelling; lower flights tend to increase the quality of the DEM (Fig. 5a). Also, flights performed under overcast conditions led to better results (Fig. 5b), most likely due to the more uniform illumination and absence of hard and moving shadows. The influences of

other flight conditions are clearly not significant; Table 4 contains the summarised statistical results.

Surprisingly, none of the quantitative metrics could have been related to the flight parameters. This may indicate that the variability of the metrics between flights with the same parameters is larger than the influence of the parameters; one can also say that the performance of the UAV is robust regarding the flight configuration. The results of these statistical models are presented in Table 5 (see also the visualisation in the supporting information). The significant result of the overcast weather condition for terrain elevation should not be over interpreted: first, only one flight was conducted under such conditions; second, the model suggests that the error is larger for overcast than for clear conditions, which is
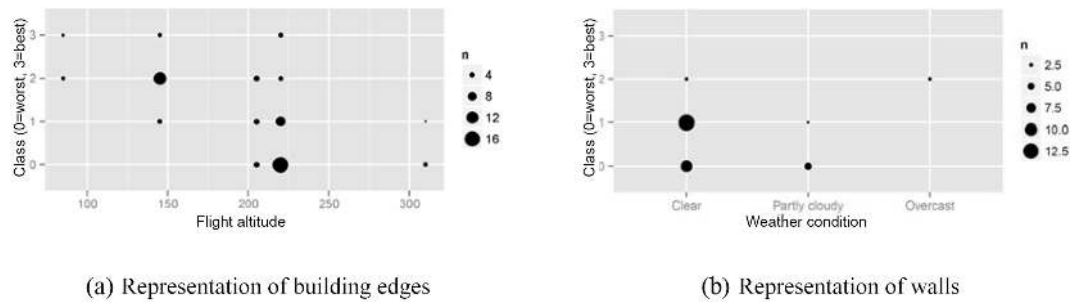
(a) Representation of building edges

(b) Representation of walls

Figure 5. Relationship between the quality of the representation of building edges and flight altitude and between wall representation and weather conditions. The size of the dots is proportional to the number of observed metrics with identical quality class and altitude or weather condition.

Table 3. Pix4D settings that were used to generate the UAV DEM.

	Assessment of influence of UAV flight parameters on DEM quality	Comparison of UAV DEM with lidar DEM
Initial processing		
Feature extraction scale	1	1
Image re-matching	No	No
Point cloud generation		
Image scale	1/2, multiscale	1/2, multiscale
Point density	One 3-D point for every 8 pixels of original image	One 3-D point for every 8 pixels of original image
Minimum matches	3	4
Point cloud filtering		
Noise filtering radius	10 GSD	14 GSD
Surface smoothing type	*Sharp*	*Medium*
Smoothing radius	10 GSD	20 GSD

counterintuitive and contradicts the result for the qualitative metrics.

Other flight parameters than the ones considered in this study may have contributed to these results; these factors could be external, such as wind conditions and time of the day, or internal, such as the camera quality and operation mode. The camera mounted in the UAV is a modified point-and-shoot consumer camera; we expect that we would have observed larger differences if a professional camera had been used. For example, a better camera could have been operated with manual exposure, settings, and would have produced more equally exposed images. This alone could have substantially improved the identification of characteristic points. These additional factors may be worth further investigations (a different experimental design) that go beyond the scope of this study.

4.2 Comparison between UAV DEM and lidar DEM

The objective of comparing the UAV DEMs and a nationwide available and commonly used DEM is to evaluate whether UAV DEMs have a similar or better quality, especially in the urban areas, which are relevant for overland flow modelling.

We expect that DEMs made available nationwide (e.g., data sets provided by Swisstopo: the Swiss Federal Office of Topography[6]) are always less accurate in the vertical dimension ($0.5 < \sigma < 1.5$ m) than the DEMs generated based on UAV imagery. Experience shows that the vertical accuracy of the latter is usually about 2 to 3 times the GSD (Pix4D Support Team, 2014), which corresponds to a standard deviation of 0.1 to 0.2 m for the DEMs of our case study.

Because the two DEMs have different resolutions and we wanted to compare the two data sets on a pixel by pixel basis, we downscaled the UAV DEM to match the resolution of the lidar DEM, using the arithmetic average to compute new pixel values.

4.2.1 Visual comparison

Qualitative (visual) assessment of DEM quality can use *hillshaded* DEMs (see Fig. 6). When looking into the whole area (Fig. 6a and b), one clear difference between the two DEMs is that around the wooded ravine (marked by 1), neither the terrain nor the trees are represented in the UAV DEM. This is due to the fact that photogrammetry is ill-suited to the high spatial complexity of the trees' branches and twigs: when captured by the drone's camera from different angles, the many overlapping elements of vegetation form complex visual patterns that are specific to each point of view and therefore cannot be matched in the photogrammetric process.

As a result, only a few areas below the vegetation can be regenerated in the photogrammetric point cloud. Because of the visual noise caused by overhead branches, the 3-D accuracy of the point cloud in these areas is compromised, which predisposes the points to be removed during the automatic point cloud filtering process. The tree-leaves-off conditions

---

[6]http://www.swisstopo.ch

Table 4. Results of the statistical models for the qualitative metrics. Bold figures represent P values below 0.05.

	Representation of voids		Representation of building edges		Representation of walls		Representation of trees	
	Estimated value	P value	Estimated value	P value	Estimated value	P value	Estimated value	P value
Flight altitude (m)	−0.00778	0.1554	−0.02531	**0.001**	−0.02950	**0.046**	−0.02685	**0.000**
Camera pitch (°)	0.00046	0.9876	0.02550	0.465	−0.09347	0.215	−0.05554	0.069
Frontal overlap (%)	−0.03073	0.4775	−0.02024	0.682	−0.01141	0.901	0.00911	0.829
Weather conditions: overcast	1.17177	0.2455	−0.37471	0.748	14.00542	**0.000**	15.03059	**0.000**
Weather conditions: partly cloudy	0.16054	0.7792	−0.53598	0.438	−1.11497	0.419	−0.44932	0.426

Table 5. Results of the statistical models for the quantitative metrics. Bold figures represent P values below 0.05.

	Terrain elevation		Curb height		Aspect		Flow path distance	
	Estimated value	P value	Estimated value	P value	Estimated value	P value	Estimated value	P value
Flight altitude (m)	0.00011	0.629	−0.00009	0.993	0.04405	0.801	0.00153	0.497
Camera pitch (°)	−0.00200	0.264	−0.00274	0.974	−1.04400	0.434	0.00213	0.903
Frontal overlap (%)	0.00032	0.800	−0.00027	0.996	−0.28786	0.759	−0.01938	0.117
Weather conditions: overcast	0.14273	**0.001**	0.00921	0.996	−15.21044	0.629	−0.16416	0.680
Weather conditions: partly cloudy	−0.00218	0.929	−0.02515	0.982	−11.16398	0.539	−0.02149	0.925

(a) UAV DEM overview (downsampled to 2 m pixel⁻¹)

(b) Lidar DEM overview (2 m pixel⁻¹)

(c) UAV DEM inset (downsampled to 2 m pixel⁻¹)
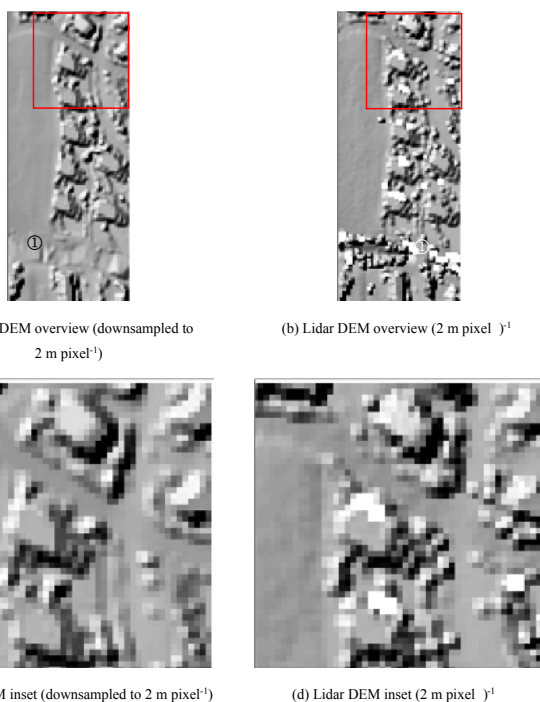
(d) Lidar DEM inset (2 m pixel⁻¹)

Figure 6. Visual comparison of the UAV DEM and lidar DEM.

during the UAV flight in early March makes it difficult to identify matching points in the canopy/on bare thin branches, which are often less wide than the GSD. In our experiments with the image data set, it was fully possible to reconstruct the tree trunks and branches of many of the trees in the above-mentioned area, but it required an image overlap far superior than what is common for cartographic photogrammetry missions. Though not having the tree canopies represented is not a problem for overland flow modelling.

Apart from differences due to the presence and better representation of vegetation in the lidar DEM, there are also mobile objects such as vehicles that differ between the two scenes.

When looking at the insets, it appears that the quality of the two DEMs is very similar, with the exception that the lidar DEM has more noise and sharper edges than the UAV DEM. This can be at least partially explained by the averaging performed when downsampling the UAV DEM.

Because the two DEMs represent different seasons, there are a number of differences between the two DEMs that are due to physical changes in the environment and not due directly to the characteristics of one DEM generation process or the other. Therefore, the comparison of the two elevation data sets using the whole area is not meaningful. Due to this fact, the comparison of the DEMs presented in the following

Figure 7. The red line polygon represents a road area selected based on visual analysis of the UAV orthophoto in order to quantitatively compare elevation, slope, and aspect of the two DEMs without the influence of objects such as vegetation, cars, or other features that are known to differ categorically between the two DEMs.

sections will be limited to a selected road area (area marked with the red line polygon in Fig. 7). This area was defined based on visual analysis of the aerial orthophoto associated to the UAV DEM. This area covers approximately 1500 m^2 and is free from cars, trees, and man-made elements such as constructions in both DEMs.

4.2.2   Elevation comparison

The map of the elevation differences between the UAV DEM and the lidar DEM (Fig. 7) was calculated subtracting the lidar DEM from the UAV DEM (Eq. 4) with 2 m pixel^{-1} resolution.

$$\Delta z_{ij} = \text{UAV}_{ij} - \text{Swisstopo}_{ij} \tag{4}$$

where Δz_{ij} is the elevation difference between the two DEMs in the cell ij, UAV_{ij} represents the elevation value of the cell ij of the UAV DEM and Swisstopo_{ij} represents the elevation value of the cell ij of the lidar DEM.

As can be seen in Fig. 8, the differences between the two DEMs in this area are almost negligible. The minimum, maximum, mean, and standard deviation of the elevation differences between the two DEMs are -0.468, 0.306, 0.06, and 0.119 m, respectively.

4.2.3   Slope and aspect comparison

The slope differences were calculated for the selected road area (see red line polygon in Fig. 6a) using (Eq. 5) with 2 m pixel^{-1} resolution.

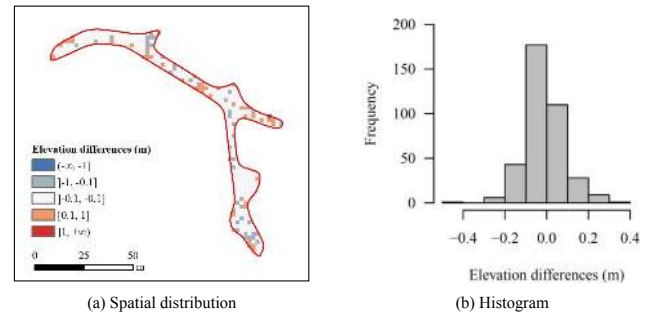$$\Delta s_{ij} = \text{UAV}_{ij} - \text{Swisstopo}_{ij}, \tag{5}$$

(a) Spatial distribution   (b) Histogram

Figure 8. Elevation differences between the UAV DEM and the lidar DEM (both with 2 m pixel^{-1} resolution).

(a) Spatial distribution   (b) Histogram
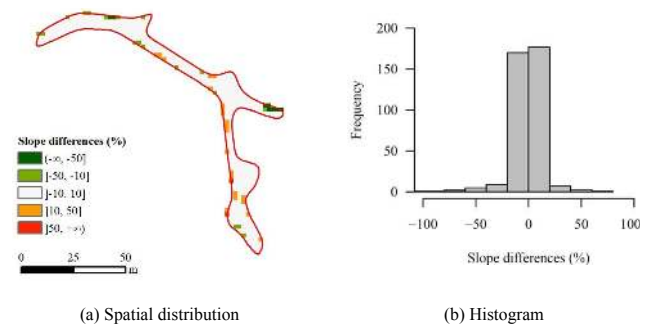
Figure 9. Slope differences between the UAV DEM and the lidar DEM.

where Δs_{ij} is the slope difference between the two DEMs in the cell ij, UAV_{ij} represents the slope value of the cell ij of the UAV DEM, and Swisstopo_{ij} represents the slope value of the cell ij of the lidar DEM.

As can be seen in Fig. 9, the slope differences between the two DEMs are almost always below 10 %; it is noteworthy that the larger slope differences are located along the boundary of the red-line polygon. The value of the descriptive statistics of the slope differences between of the two DEM are

 – minimum: -115.64 %;

 – maximum: 74.41 %;

 – mean: -0.86 %;

 – standard deviation: 14.16 %.

The terrain aspect distribution of the selected road area of the two DEMs is also very similar, as presented in Fig. 10.

4.2.4   Delineation of flow paths

Flow paths were delineated using the conventional D8 flow direction algorithm (Jenson and Domingue, 1988) for the three UAV DEMs at different resolutions (0.5, 1.0 and 2.0 m pixel^{-1}) as well as for the lidar DEM. The results are presented in Fig. 11 and show that the flow paths delineated
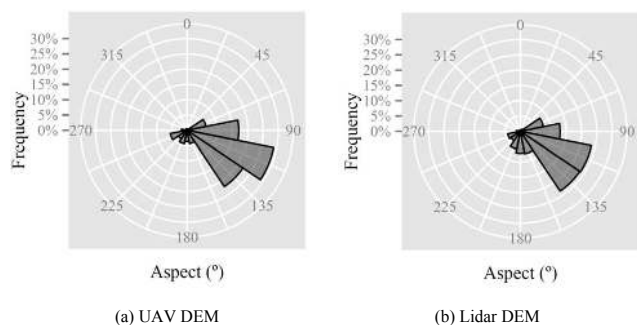
(a) UAV DEM

(b) Lidar DEM

Figure 10. Distribution of terrain aspect. The aspect values are in degrees. The outer number represent the cardinal directions in degrees.

using the UAV DEMs followed a realistic path along the side of the road. This behaviour was retained even when the UAV DEM was downsampled to $2\,\text{m pixel}^{-1}$ (Fig. 11c); this is in close agreement with the results presented by Sampson et al. (2012), who downsampled terrestrial lidar for use in urban inundation models. In comparison to the lidar DEM, it is clearly seen that the UAV DEMs can add additional detail to overland flow modelling applications; flow paths obtained using the lidar DEM are slightly different from the ones obtained using the UAV-based DEM.

5 Conclusions

In this study, we demonstrate the applicability and the advantages of using UAVs to generate very high resolution DEMs to be used in urban overland flow and flood modelling. To address this objective, we assessed (i) the influence of flight parameters in the quality of the DEMs produced using UAVs technology, and (ii) the quality of the UAV-based DEM in comparison to the conventional lidar-based DEM available in Switzerland. We concluded that

– UAV platforms and software are a mature technology that deliver basic data leading to satisfactory results for urban overland flow modelling.

– Interestingly, only few dependencies between the flight parameters and DEM quality could be identified. This might be due to variability introduced by other external and internal factors not investigated in detail in this study. Although, at first sight, this might leave only little potential for optimal experimental design, at second sight this also means that the technology is rather robust against flight altitude, camera pitch settings, image overlapping parameters and thus suitable for practitioners.

– As expected, the most influential flight parameter was the flight altitude, where *lower flights* produce better DEMs. Other flight parameter, such as the effect of sun
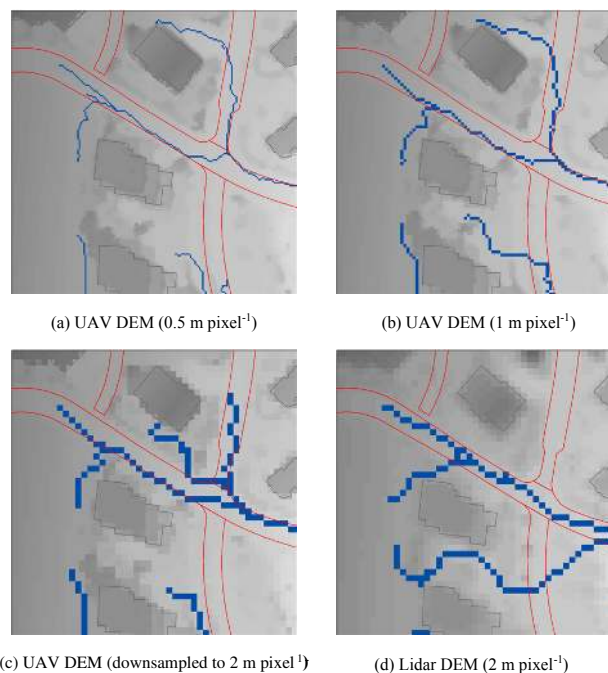

(a) UAV DEM (0.5 m pixel^{-1})

(b) UAV DEM (1 m pixel^{-1})

(c) UAV DEM (downsampled to 2 m pixel^{-1})

(d) Lidar DEM (2 m pixel^{-1})

Figure 11. DEM-based flow path delineation.

(e.g., weather conditions), showed some effect on the DEM quality but its effect was clearly weaker than the flight altitude – *overcast weather conditions* are better. Other relationships could not be observed as hypothesised, e.g. camera pitch and image overlapping. For a given flight parameter, the number of samples (flights) may have been a limiting factor to observe trends. In future studies, it would be recommended to conduct additional flight campaigns. By repeating flights with the same parameters in order to quantify how much DEM quality may vary, independently of flight parameters one may also evaluate uncertainty in the elevation data generated. Additional flight parameters may also be considered in future studies, such as the time of day.

– Comparing the UAV DEM to a commonly available lidar-based DEM, we found that the quality of both DEMs is comparable. The differences between the two DEMs are not substantial, especially when the comparison is conducted in a selected road area without cars, buildings, trees, or vegetation. When comparing flow paths delineated using the different DEMs, it could be seen that the flow paths obtained using a DEM downsampled (2 m pixel size) from the finer resolution UAV DEM (0.05 m pixel size) retained the major flow path patterns. The flow paths obtained using the lidar DEM were slightly different from those obtained using the UAV DEMs; this is mostly due to the presence of vegetation and trees in the first DEM. The UAV DEM has two main/practical advantages over the lidar DEM, de-

www.hydrol-earth-syst-sci.net/20/1637/2016/

Hydrol. Earth Syst. Sci., 20, 1637–1653, 2016

spite the similarities mentioned above. First, it is more flexible to acquire elevation data using UAVs, especially for small to medium size areas (or catchments), and the second is that if the UAV flights are conducted during winter with tree-leaves-off conditions, DEMs with no tree canopies represented can be produced, which are especially beneficial for land use classification and overland flow processes. It is, however, important to mention that there are other solutions to generate DEMs other than nationwide airborne lidar-based and UAV-based solutions, such as ground-based lidar. In particular, a ground-based lidar solution is as flexible as the UAV solution, capable of producing very fine resolution DEMs and may not have the problem of obstruction by tree leaves as photogrammetric mini UAV solutions. However, it also has disadvantages: the major one is perhaps related to the limitation of covering areas located behind the buildings, i.e. it does not allow for covering the whole area of interest (e.g. an urban catchment).

– Our findings suggest that UAVs can greatly improve overland flow modelling by increasing the detail of terrain representation and also by their inherent flexibility to update existing elevation data sets. The very high resolution that is possible to obtain using UAV DEMs is also an advantage for urban overland flow and flood modelling purposes. Further research should be carried out towards the development of an urban drainage modelling application in order to assess the real benefit of using very high resolution DEMs and hydraulic models.

In addition to the generation of DEMs, UAV imagery can also be used to generate other very interesting data sets for urban drainage modelling applications based on image classification. These are, for example, identification of pervious/impervious areas (Tokarczyk et al., 2015), automatic identification and location of sewer inlets and manholes, and other man-made features relevant to overland flow (Moy de Vitry, 2014).

Appendix A: Unmanned aerial system

The mini UAV platform used in the study is a fully autonomous fixed-wing aircraft developed by senseFly SA[7]. The UAV is electric powered, has a wingspan of 0.96 m, and weighs approximately 0.7 kg including a payload of 0.15 kg. The UAV can cover large areas in a reasonable amount of time, which is important for the economic viability of UAV remote sensing. Detailed information is provided in Table A1.

The specifications of the IXUS 127 HS camera part of the unmanned aerial system used in this study are presented in Table A2.

Table A1. Detailed characteristics of the UAV.

Wingspan	0.96 m
Wing area	0.25 m
Typical weight	0.7 kg
Payload	16 MP camera, electronically integrated and controlled
Battery	3-cell lithium-polymer
Capacity	1800 mAh
Endurance	45 min of flight time
Propulsion	electric brushless motor
Nominal cruise speed	36–72 km h^{-1} (10–20 m s^{-1})
Wind resistance	up to 45 km h^{-1} (12 m s^{-1})
Mapping area	coverage up to 10 km^2
Remote control	2.4 GHZ, range: approx. 1 km, certification: CE. FCC
Data communication	2.4 GHZ, range: approx. 3 km, certification: FCC Part 15.247
Navigation	autonomous flight and landing, up to 50 waypoints direction
Material	styrofoam
Cost (in 2015)	approx. CHF 20 000 (UAV + camera + software)

Table A2. Specifications of the Canon IXUS 127 HS.

Camera effective pixels	approx. 16.1 million pixels
Lens focal length	5 × zoom: 4.3 (W)–21.5 (T) mm
	(35 mm film equivalent: 24 (W)–120 (T) mm)
File formats	Exif 2.3 (JPEG)
Dimensions	93.2 × 57.0 × 20.0 mm (based on CIPA Guidelines)
Weight	approx. 0.135 kg (including batteries and memory card)

---

[7]http://www.sensefly.com

The Supplement related to this article is available online at doi:10.5194/hess-20-1637-2016-supplement.

References

Allitt, R., Blanksby, J., Djordjevic, S., Maksimovic, C., and Stewart, D.: Investigations into 1D-1D and 1D-2D Urban Flood Modelling, in: WaPuG Autumn conference, 11–13 November 2009, Blackpool, UK, 2009.

Apel, H., Aronica, G. T., Kreibich, H., and Thieken, A. H.: Flood Risk Analyses – how Detailed Do We Need to Be?, Nat. Hazards, 49, 79–98, doi:10.1007/s11069-008-9277-8, 2009.

Baltsavias, E.: A Comparison between Photogrammetry and Laser Scanning, ISPRS J. Photogram. Remote Sens., 54, 83–94, doi:10.1016/S0924-2716(99)00014-3, 1999.

Bennett-Jones, O.: Searching for a New Name for Drones, BBC News, http://www.bbc.com/news/magazine-25979068 (last access: 23 April 2015), 2014.

Burrough, P. A. and McDonnell, R. A.: Principles of Geographical Information Systems, Oxford University Press, New York, 1998.

Chen, A. S., Djordjević, S., Leandro, J., and Savić, D.: The urban inundation model with bidirectional flow interaction between 2D overland surface and 1D sewer networks, in: Novatech, Lyon, France, 465–472, 2007.

Colomina, I. and Molina, P.: Unmanned Aerial Systems for Photogrammetry and Remote Sensing: A Review, ISPRS J. Photogram. Remote Sens., 92, 79–97, doi:10.1016/j.isprsjprs.2014.02.013, 2014.

De Jong, S. M., Hornstra, T., and Maas, H.: An integrated spatial and spectral approach to the classification of Mediterranean land cover types: the SSC method, Int. J. Appl. Earth Obs. Geoinf., 3, 176–183, 2001.

Duives, D. C., Daamen, W., and Hoogendoorn, S.: Trajectory Analysis of Pedestrian Crowd Movements at a Dutch Music Festival, in: Pedestrian and Evacuation Dynamics 2012, edited by: Weidmann, U., Kirsch, U., and Schreckenberg, M., Springer International Publishing, Cham, Switzerland, 151–166, doi:10.1007/978-3-319-02447-9_11, 2014.

Eisenbeiss, H.: UAV Photogrammetry, ETH Zürich Inst. f. Geodäsie u. Photogrammetrie, Zürich, 2009.

Fewtrell, T. J., Duncan, A., Sampson, C. C., Neal, J. C., and Bates, P. D.: Benchmarking Urban Flood Models of Varying Complexity and Scale Using High Resolution Terrestrial LiDAR Data, Phys. Chem. Earth A/B/C, 36, 281–291, doi:10.1016/j.pce.2010.12.011, 2011.

Jenson, S. K. and Domingue, J. O.: Extracting Topographic Structure from Digital Elevation Data for Geographic Information System Analysis, Photogram. Eng. Remote Sens., 54, 1593–1600, 1988.

Kraus, K.: Band 1 Photogrammetrie, Geometrische Informationen aus Photographien und Laserscanneraufnahmen, De Gruyter, Berlin, Boston, http://www.degruyter.com/view/product/61449 (last access: 26 April 2016), 2012.

Leandro, J., Djordjević, S., Chen, A., and Savić, D. A.: Flood inundation maps using an improved 1D/1D model, in: 8th UDM: International Conference on Urban Drainage Modelling, 7–12 September 2009, Tokyo, Japan, 2009.

Leberl, F., Irschara, A., Pock, T., Meixner, P., Gruber, M., Scholl, S., and Wiechert, A.: Point Clouds: LIDAR versus 3D Vision, Photogram. Eng. Remote Sens., 76, 1123–1134, 2010.

Leitão, J. P., Boonya-Aroonnet, S., Prodanovic, D., and Maksimovic, C.: The influence of digital elevation model resolution on overland flow networks for modelling urban pluvial flooding, Water Sci. Technol., 60, 3137–3149, doi:10.2166/wst.2009.754, 2009.

Maksimović, Č., Prodanović, D., Boonya-aroonnet, S., Leitão, J. P., Djordjević, S., and Allitt, R.: Overland flow and pathway analysis for modelling of urban pluvial flooding, J. Hydraul. Res., 47, 512–523, doi:10.1080/00221686.2009.9522027, 2009.

Montgomery, D. C., Peck, E. A., and Vining, G. G.: Introduction to Linear Regression Analysis, Wiley, Hoboken, NJ, 2012.

Moy de Vitry, M.: Improving urban flood management with autonomous mini-UAVs, MSc thesis, ETH Zurich, Zurich, Switzerland, 2014.

Pix4D Support Team: Pix4D Knowledge Base, Pix4D Support, https://support.pix4d.com/entries/26825498, last access: 27 April 2015, archived by WebCite at: http://www.webcitation.org/6Y6TNZI2U (last access: 26 April 2016), 2014.

Podobnikar, T.: Methods for Visual Quality Assessment of a Digital Terrain Model, S.A.P.I.EN.S. Surveys and Perspectives Integrating Environment and Society, http://sapiens.revues.org/738 (last access: 26 April 2016), 2009.

Reinartz, P., d' Angelo, P., Krauß, T., Poli, D., Jacobsen, K., and Buyuksalih, G.: Benchmarking and Quality Analysis of Dem Generated from High and Very High Resolution Optical Stereo Satellite Data, in: Proceedings of the The 2010 Canadian Geomatics Conference and Symposium of Commission I, ISPRS Convergence in Geomatics – Shaping Canada's Competitive Landscape, Calgary, Alberta, Canada, available at: http://www.isprs.org/proceedings/XXXVIII/part1/09/09_03_Paper_33.pdf (last access: 26 April 2016), 2010.

Remondino, F., Barazzetti, L., Nex, F., Scaioni, M., and Sarazzi, D.: UAV Photogrammetry for Mapping and 3d Modeling–current Status and Future Perspectives, International Archives of the Photogrammetry, Remote Sensing and Spatial Information Sciences, Zurich, Switzerland, 38, 25–31, 2011.

Sampson, C. C., Fewtrell, T. J., Duncan, A., Shaad, K., Horritt, M. S., and Bates, P. D.: Use of Terrestrial Laser Scanning Data to Drive Decimetric Resolution Urban Inundation Models, Adv. Water Resour., 41, 1–17, doi:10.1016/j.advwatres.2012.02.010, 2012.

Sauerbier, M. and Eisenbeiss, H.: UAVs for the Documentation of Archaeological Excavations, International Archives of Photogrammetry, Remote Sensing and Spatial Information Sciences, Newcastle upon Tyne, UK, 526–531, 2010.

Sona, G., Pinto, L., Pagliari, D., Passoni, D., and Gini, R.: Experimental Analysis of Different Software Packages for Orientation and Digital Surface Modeling from UAV Images, Earth Sci. Inform., 7, 97–107, doi:10.1007/s12145-013-0142-2, 2014.

Strecha, C., Gervaix, F., Fua, P., Zufferey, J.-C., Beyeler, A., Floreano, D., and Küng, O.: The Accuracy of Automatic Photogrammetric Techniques on Ultra-Light UAV Imagery, in: UAV-g 2011 – Unmanned Aerial Vehicle in Geomatics, Zurich, Switzerland, available at: http://infoscience.epfl.ch/record/168806 (last access: 26 April 2016), 2011.

Tokarczyk, P., Leitao, J. P., Rieckermann, J., Schindler, K., and Blumensaat, F.: High-quality observation of surface imperviousness for urban runoff modelling using UAV imagery, Hydrol. Earth Syst. Sci., 19, 4215–4228, doi:10.5194/hess-19-4215-2015, 2015.

Triggs, B., McLauchlan, P. F., Hartley, R. I., and Fitzgibbon, A. W.: Bundle Adjustment – A Modern Synthesis, in: Vision Algorithms: Theory and Practice, Lecture Notes in Computer Science 1883, edited by: Triggs, B., Zisserman, A., and Szeliski, R., Springer, Berlin, Heidelberg, doi:10.1007/3-540-44480-7_21, 2000.

VBS: Technische Verordnung Des VBS Über Die Amtliche Vermessung, http://www.admin.ch/opc/de/classified-compilation/19940126/200807010000/211.432.21.pdf (last access: 23 April 2015), 2008.

Venables, W. N. and Ripley, B. D.: Modern Applied Statistics with S, Springer, New York, 2002.

Villanueva, I., Pender, G., Lin, B., Mason, D. C., Falconer, R. A., Neelz, S., Crossley, A. J., and Mason, D. C.: Benchmarking 2D Hydraulic Models for Urban Flooding, Proc. ICE-Water Manage., 161, 13–30, doi:10.1680/wama.2008.161.1.13, 2008.

Vilmer, J.-B.: Armed drones and target killings: legal and ethical challenges, in: Drones: From Technology to Policy, Security to Ethics, Forum, 30 January 2015, ETH Zurich, Switzerland, 2015.

Vojinovic, Z. and Tutulic, D.: On the use of 1D and coupled 1D–2D modelling approaches for assessment of flood damages in urban areas, Urban Water J., 6, 183–199, 2009.

Wildi, J.: Drones: industry and business applications, in: Drones: From Technology to Policy, Security to Ethics, Forum, 30 January 2015, ETH Zurich, Switzerland, 2015.

Zhang, C. and Kovacs, J. M.: The Application of Small Unmanned Aerial Systems for Precision Agriculture: A Review, Precis. Agricult., 13, 693–712, doi:10.1007/s11119-012-9274-5, 2012.